31st Annual International Conference of the IEEE EMBS
Minneapolis, Minnesota, USA, September 2-6, 2009

Extracellular Stimulation of Mouse Retinal Ganglion Cells with Non-Rectangular Voltage-Controlled Waveforms

Donald R Cantrell, and John B Troy

Abstract—**Neural prostheses rely upon electric stimulation to control neural activity. However, electrode corrosion and tissue damage may result from the injection of high charge densities. During electrical stimulation with traditional voltage-controlled square-wave pulses, the current density distribution on the surface of the stimulating electrode is highly nonuniform, with the highest current densities located at the edge of disk-shaped electrodes. Current density is implicated in tissue damage and electrode corrosion because it determines the charge density distribution. Through recent computer modeling work, we have found that Gaussian and sinusoidal stimulus waveforms produce a current density distribution that is significantly more uniform than the one produced by square-wave pulses. In this manner, these non-rectangular waveforms reduce the peak current densities without decreasing the efficacy of the neural stimulus. In the present work, we utilize an *in vitro* mouse retinal preparation to compare the same set of alternative stimulus waveforms. The -1V amplitude voltage-controlled stimuli were delivered through 20 μm diameter titanium nitride electrodes. Importantly, when normalized for the amount of injected charge, the data demonstrate that each waveform is similarly effective at eliciting a neural response. Also, the suprathreshold Gaussian and sinusoidal waveforms possessed much lower peaks in current. For this reason, these non-rectangular waveforms may be useful in reducing electrode corrosion and tissue damage.**

I. Introduction

THE electric stimulation of neural tissue allows neuroprosthetic devices to control neural activity. Electric stimulation, however, can cause tissue damage. McCreery and his colleagues have demonstrated that both charge density and charge per stimulus phase contribute to damage [1], a conclusion that is now widely accepted by the neural stimulation community [2-4]. In these works, charge density per phase was calculated by dividing charge per phase by the geometric surface area of the electrode, with the implicit assumption that the current density distribution on the electrode surface was uniform. Shannon analyzed the data generated by McCreery et al and concluded that the threshold for the safe amount of charge capable of being injected through an electrode was proportional to the radius of the electrode, and not to its surface area [5]. Shannon then hypothesized that this was due to the focusing of current at the perimeter of the disk electrodes, a phenomenon often referred to as the edge effect.

In a seminal series of works, Newman derived an analytical solution for the current density distribution on the surface of a disk electrode submersed in a resistive medium with no electrode-electrolyte interfacial impedance [6]. The current density distribution that he described was highly nonuniform, with the largest current densities crowded at the perimeter of the electrode, and this has been termed the primary distribution. Next, Newman incorporated resistive and capacitive elements into the electrode-electrolyte interface and demonstrated that a much more uniform secondary current density distribution may be established if the impedance to current flow is relatively large compared to the solution resistance [7, 8]. Nisancioglu and Newman then considered the transient response of a disk electrode to steps in voltage and current, and they described the progression of the current density from the primary distribution to the secondary distribution as the voltage drop at the electrode-electrolyte interface was increased [9, 10]. These works demonstrated that the current density distribution is greatly influenced by the electrode-electrolyte interfacial impedance, and that the edge effect is most pronounced when this impedance is small.

Relevant to the field of neural engineering, the impedances of Pt, TiN, and IrO_x electrodes in physiological saline have been thoroughly studied [11-13]. In general, the impedances of these electrodes decrease at large overpotentials and high frequencies.

Based on Shannon's observation, it may be possible to improve tissue tolerance of stimulating electrodes by reducing the nonuniformity of the current density distribution. Several groups have described alternative electrode geometries designed to reduce peak current densities and create uniform distributions on the surface of stimulating electrodes [14-16]. Alternatively, because the current density distribution is dependent upon the electrode-electrolyte interfacial impedance, and because this impedance is determined by frequency and overpotential, it may be possible to create more uniform current density distributions by controlling the stimulus waveform. Despite the fact that the first published charge balanced biphasic current-controlled stimulus waveform was non-rectangular [17], current protocols generally utilize rectangular pulses. Non-rectangular pulses have only recently regained attention [18]. Our previous work with finite element models of neural electric stimulation compared the efficacy and current density distribution achieved with square, Gaussian, and sinusoidal voltage-controlled waveforms. The results suggested that, compared to square waveforms, stimulation

Manuscript received March 7, 2009. This work was supported by NIH R21 EB004200. DRC was supported in part by 1 TL 1 RR 025739-01, an NIH CTSA awarded to Northwestern University.

D. R. Cantrell is with Northwestern University Interdepartmental Neuroscience Program, Northwestern University, Evanston, IL 60208 USA (email: Cantrell@md.northwestern.edu).

J. B. Troy is with the Department of Biomedical Engineering, Northwestern University, Evanston, IL 60208 USA (phone: 847-491-3822; email: j-troy@northwestern.edu).

with Gaussian and sinusoidal waveforms may demonstrate more uniform current density distributions and reduced peak current densities without a significant change in stimulus efficacy [19]. Efficacy was defined by the amount of charge required to elicit a neural response. In the present work, we utilize an *in vitro* mouse retinal preparation to compare the efficacies of these alternative waveforms and the peak currents that they generate.

II. Methods

Mice ranging from post-natal day 20 to 25 were euthanized in accordance with the Northwestern University IACUC. The retina was isolated and placed ganglion cell side down onto an array of hexagonally packed titanium nitride (TiN) electrodes with diameters ranging from 10 to 30 μm [HexaMEA, Multichannel Systems, Germany]. The retina was held in place with a small manipulator, and the system was perfused with an oxygenated artificial cerebrospinal fluid. With this retinal preparation, we can routinely record the spike trains of more than 50 retinal ganglion cells for a duration exceeding 8 hours. A more detailed description of the retinal preparation can be found elsewhere [20].

Voltage recordings from each electrode of the array were preamplified [1060-BC Multichannel Systems, Germany] and digitized at 25 kHz. In order to reduce the stimulus artifact, the preamplifier contains a blanking circuit, which allows the recording circuitry to be isolated while stimuli are delivered to the individually addressable electrodes. Voltage-controlled stimuli were generated digitally with 20 μs timesteps using the STG 1002 stimulus generator [Multichannel Systems, Germany]. The stimulus was applied through a 75 kOhm test resistance placed in series with the stimulating electrode. Current was determined by measuring the voltage drop across this test resistor, which was accomplished with a custom Labview program sampling at 100 kHz.

Rectangular, Gaussian, and sinusoidal waveforms were studied. The sinusoidal pulse was a half period sine wave truncated at 0 and 180 degrees. The width of the Gaussian stimulus was considered to be the time inside three standard deviations around the peak. All stimuli were –1V in amplitude, and they were varied only in their duration. Rectangular stimuli ramping up in duration from 200 μs to 1000 μs in 40 μs steps were the first to be applied to the retina. Each duration was repeated six times, and four seconds elapsed between each pulse. This was followed by incrementing sinusoidal stimuli and then Gaussian stimuli. Next, decrementing rectangular, sinusoidal, and Gaussian stimuli were delivered to the electrode using the same pulse durations. Following this protocol, a total of twelve stimuli for each combination of waveform and duration were delivered to the retina. The neural responses were averaged over all twelve stimulus instances. Despite the 1 ms hardware blanking, a significant stimulus artifact remained in the recording. This artifact was further suppressed by the offline implementation of the SALPA algorithm [21].

After removal of the artifact, spikes were identified by voltage threshold. Spikes within 30 ms of the stimulus were counted. Most spikes occurred in the 5 to 20 ms time period following the stimulus. These are long latency spikes, and short latency spikes (<2 ms) could not be resolved here [22]. Because these experiments were designed to compare alternative stimulus waveforms, and not to identify the threshold for individual cell responses, spike sorting was not performed. Nonetheless, most channels contained only one stimulus-responsive cell. Figure 1 shows examples of raw voltage recordings.

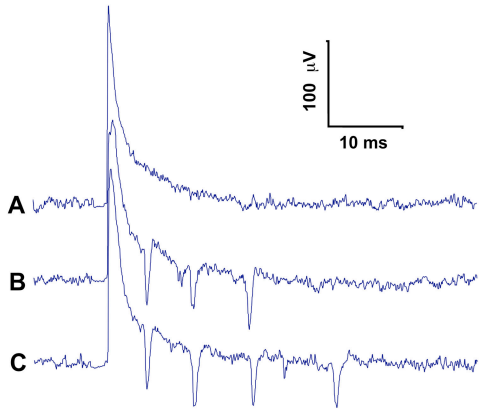

Fig. 1. Raw voltage recordings from a TiN electrode 60 μm from the stimulating electrode. Trace A demonstrates the lack of neural response to a 480 μs sinusoidal pulse. Trace B shows three action potentials responding to a 760 μs sinusoidal pulse, and trace C demonstrates four action potentials responding to a 1000 μs sinusoidal pulse.

III. Results

The strength of the response, as measured by the number of spikes was plotted against both the stimulus duration and the injected charge for the three waveforms. Due to the capacitive nature of the TiN electrode-electrolyte interface, the monophasic voltage waveforms create biphasic current waveforms. The injected charge was calculated by integrating the recorded current over the course of the cathodic phase of the stimulus. Figure 2 plots a representative channel. At -1 nC monophasic injected charge, the raw response strengths of the alternative waveforms were compared to the square response strengths using matched t-tests. Also, for comparison, the response strengths elicited by the sinusoidal and Gaussian waveforms were normalized against the response strengths for the square waveform. Response strengths were generally similar among the three waveforms. Nonetheless, at –1 nC both the alternative waveforms trended toward greater efficacy than the square waveform. The normalized sinusoidal response strength at –1 nC was 115% that of the square with 6% SEM (p-value = 0.0417). The normalized Gaussian response was 125% that of the square with 28% SEM (p-value = 0.2054). A total of 6 electrode channels were analyzed in 3 different mouse retinas. Comparisons were made at -1 nC because this amount of charge was delivered by all three waveforms,

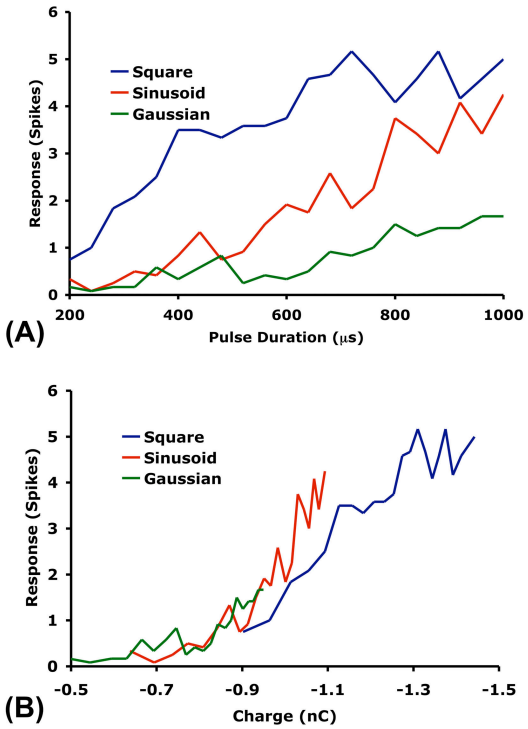

Fig. 2. Representative neural response plotted against (A) duration and (B) charge. Alternative stimulus waveforms were applied to a 20 μm diameter TiN electrode. In panel A, the number of elicited action potentials were counted, and plotted against the stimulus duration. In panel B, the neural response is plotted against the amount of cathodal injected charge, which was calculated by integrating the current over the cathodic phase of the waveform.

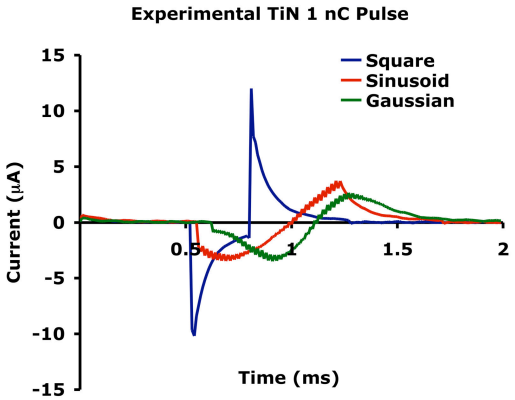

Fig. 3. Current waveforms generated by square, sinusoidal, and Gaussian voltage-controlled stimuli. Each waveform injects 1 nC of cathodic current. The voltage waveforms were all –1V in amplitude, and they were delivered to a 20 μm diameter TiN electrode to stimulate the mouse retina. The square voltage waveform was 280 μs in duration. The sinusoidal voltage waveform was 720 μs, and the Gaussian waveform was 1000 μs in duration. The greatest peaks in current are delivered by the square waveform.

and because at this stimulus strength, the neural response was not yet saturated.

In contrast, the peak currents delivered by these alternative waveforms are drastically different. Figure 3 plots the time course of the current during stimulation. Each stimulus delivers 1 nC of cathodic charge, and thus elicits a similar neural response. The square voltage-controlled waveform delivers much greater peak currents to the stimulating electrode at the beginning and the end of the voltage waveform. The peak current density of the square waveform is 3.2 times larger than the peak current density of the sinusoidal waveform and 3.5 times larger than that of the Gaussian waveform.

IV. Discussion

The results demonstrate that for stimuli of a fixed voltage amplitude, Gaussian and sinusoidal waveforms can achieve the desired neural response while reducing peak currents delivered to the stimulating electrode. During these experiments, the current waveforms were recorded, but the current density distribution on the surface of the electrode could not be directly observed. However, analytical and computational models of neural stimulation suggest that the current density will be most intensely focused in regions of high curvature when the impedance to the flow of current is low [7, 8, 23, 24]. Thus, the largest peaks in current plotted in Figure 3 are likely accompanied by the most highly nonuniform current density distributions. Therefore, of the three waveforms, these data strongly suggest that the square waveform delivers the largest current densities.

Importantly however, it is not clear from these data whether the *charge* delivered by the square waveform is more intensely focused to the perimeter of the stimulating disk electrode than the charge delivered by the Gaussian and sinusoidal waveforms. Although the current delivered by the square waveform contains the largest peaks, its magnitude quickly decreases to levels below the broader peaks of the alternative waveforms. Following the argument in the previous paragraph, each current phase of the monophasic voltage-controlled square waveform initiates with a period of highly nonuniform current density and is followed by a period characterized by a relatively uniform distribution. This progression from a primary distribution to a secondary distribution for a voltage step has been described analytically [10]. Because the square stimulus contains periods in which the current density distribution is likely to be both more uniform and less uniform than the distributions created by the Gaussian and sinusoidal waveforms, it cannot be determined from these data whether the spatial delivery of charge differs for the three waveforms. This has become an important focus of our future work.

In this paper, we focused on voltage-controlled waveforms. We reasoned that the safety limitations of electrical stimulation are fundamentally tied to the electrochemical reactions allowed to occur at the electrode-tissue interface [2]. The available electrochemical reactions are determined by the overpotential, and at low

overpotentials current is passed in a safer, more reversible manner, which is primarily capacitive for TiN. The overpotential can be most directly limited by utilizing voltage-controlled waveforms, and therefore we believe that voltage-control, if implemented properly, will offer the safest strategy. Notably, an alternative theory hypothesizes that tissue damage is caused by neural hyperexcitation [25].

Current-controlled charge-balanced rectangular biphasic waveforms are now perhaps the most popular choice in electrical stimulation. It is important to emphasize therefore, that due to the capacitive nature of the TiN microelectrodes, the monophasic voltage-controlled waveforms utilized in this work generate biphasic current waveforms that are very nearly charged balanced. For example, in Figure 3, the net injected charge for the square wave is -0.031 nC. For the sinusoid, it is -0.029 nC, and for the Gaussian waveform, it is -0.070 nC. Additionally, despite the fact that square current-controlled waveforms maintain a constant spatially averaged current during each phase of the stimulus, the current density distribution on the surface of the electrode will undergo an evolution from a highly nonuniform distribution to a more uniform one in a manner very similar to what has been described in this paper for square voltage pulses [9]. This changing current density distribution is again caused by a changing electrode-electrolyte impedance, but in the case of a current-controlled stimulus, the changing impedance is evidenced by the non-rectangular voltage waveform created during the stimulus.

V. Conclusion

We utilized an *in vitro* mouse retinal preparation to study the electrical stimulation of neural tissues with alternative voltage-controlled waveforms. We compared –1V amplitude rectangular, Gaussian, and sinusoidal stimulus waveforms of varying duration. Most importantly, the data show that for a given injected charge, the waveforms elicit neural responses of similar strength. The data show a trend suggesting that the non-rectangular waveforms are slightly more effective. Additionally, for suprathreshold stimuli, the Gaussian and sinusoidal waveforms demonstrated smaller peaks in current than the rectangular stimulus. This observation strongly suggests that the Gaussian and sinusoidal stimulus waveforms deliver much smaller peak current densities than the square stimulus, and for this reason the alternative waveforms may help to reduce electrode corrosion and tissue damage. However, because the current density distribution could not be directly observed, it is unclear whether the *charge* distribution differs for the three suprathreshold stimulus waveforms.

References

[1] D. McCreery, W. Agnew, T. Yuen, and L. Bullara, "Charge density and charge per phase are cofactors in neural injury induced by electrical stimulation," *IEEE Trans. Biomed. Eng.,* vol. 37, pp. 996-1001, 1990.

[2] S. Cogan, "Neural stimulation and recording electrodes," *Annu. Rev. Biomed. Eng.,* vol. 10, pp. 275-309, 2008.

[3] D. Merrill, M. Bikson, and J. Jeffreys, "Electrical stimulation of excitable tissue: design of efficacious and safe protocols," *J. Neurosci. Methods,* vol. 141, pp. 171-198, 2005.

[4] E. Tehovnik, "Electrical stimulation of neural tissue to evoke behavioral responses," *J. Neurosci. Methods,* vol. 65, pp. 1-17, 1996.

[5] R. Shannon, "A model of safe levels for electrical stimulation," *IEEE Trans. Biomed. Eng.,* vol. 39, pp. 424-426, 1992.

[6] J. Newman, "Resistance for flow of current to a disk," *J. Electrochem. Soc.,* vol. 113, pp. 502-502, 1966.

[7] J. Newman, "Current distribution on a rotating disk below the limiting current," *J. Electrochem. Soc.,* vol. 113, pp. 1235-1241, 1966.

[8] J. Newman, "Frequency dispersion in capacity measurements at a disk electrode," *J. Electrochem. Soc.,* vol. 117, pp. 198-203, 1970.

[9] K. Nisancioglu and J. Newman, "Transient response of a disk electrode," *J. Electrochem. Soc.,* vol. 120, pp. 1339-1346, 1973.

[10] K. Nisancioglu and J. Newman, "Transient response of a disk electrode with controlled potential," *J. Electrochem. Soc.,* vol. 120, pp. 1356-1358, 1973.

[11] R. Meyer, S. Cogan, T. Nguyen, and R. Rauh, "Electrodeposited iridium oxide for neural stimulation and recording electrodes," *IEEE Trans. Neural Syst. Rehabil. Eng.,* vol. 9, pp. 2-11, 2001.

[12] A. Richardot and E. McAdams, "Harmonic analysis of low-frequency bioelectrode behavior," *IEEE Trans. Med. Imaging,* vol. 21, pp. 604-612, 2002.

[13] J. Weiland, D. Anderson, and M. Humayun, "*In vitro* electrical properties for iridium oxide versus titanium nitride stimulating electrodes," *IEEE Trans. Biomed. Eng.,* vol. 49, pp. 1574-1579, 2002.

[14] D. Ksienski, "A minimum profile uniform current density electrode," *IEEE Trans. Biomed. Eng.,* vol. 39, pp. 682-692, 1992.

[15] J. Rubinstein, F. Spelman, M. Soma, and M. Suesserman, "Current density profiles of surface mounted and recessed electrodes for neural prostheses," *IEEE Trans. Biomed. Eng.,* pp. 864-875, 1987.

[16] S. Tungjitkusolmun, E. Woo, H. Cao, J. Tsai, V. Vorperian, and J. Webster, "Finite element analyses of uniform current density electrodes for radio-frequency cardiac ablation," *IEEE Trans. Biomed. Eng.,* vol. 47, pp. 32-40, 2000.

[17] J. Lilly, J. Hughes, E. Alvord, and T. Galkin, "Brief, noninjurious electric waveform for stimulation of the brain," *Science,* vol. 121, pp. 468-469, 1955.

[18] M. Sahin and Y. Tie, "Non-rectangular waveforms for neural stimulation with practical electrodes," *J. Neural Eng.,* vol. 4, pp. 227-233, 2007.

[19] D. Cantrell and J. Troy, "A time domain finite element model of extracellular neural stimulation predicts that non-rectangular stimulus waveforms may offer safety benefits," in *IEEE-EMBS Annual Meeting Conference Proceedings* Vancouver, BC, Canada, 2008.

[20] L. Pinto, M. Vitaterna, K. Shimomura, S. Siepka, E. McDearmon, V. Balannik, C. Omura, S. Lumayag, B. Invergo, B. Glawe, D. Cantrell, S. Inayat, M. Olvera, K. Vessey, M. McCall, D. Maddox, C. Morgans, B. Young, M. Pletcher, R. Mullins, J. Troy, and J. Takahashi, "Generation, identification and functional characterization of the nob4 mutation of Grm6 in the mouse," *Visual Neurosci.,* vol. 24, pp. 111-123, 2007.

[21] D. Wagenaar and S. Potter, "Real-time multi-channel stimulus artifact suppression by local curve fitting," *J. Neurosci. Methods,* vol. 120, pp. 13-120, 2002.

[22] C. Sekirnjak, P. Hottowy, A. Sher, W. Dabrowski, A. Litke, and E. Chichilnisky, "Electrical stimulation of mammalian retinal ganglion cells with multielectrode arrays," *J. Neurophysiol.,* vol. 95, pp. 3311-3327, 2006.

[23] D. Cantrell, S. Inayat, A. Taflove, R. Ruoff, and J. Troy, "Incorporation of the electrode-electrolyte interface into finite element models of metal microelectrodes," *J. Neural Eng.,* vol. 5, pp. 54-67, 2008.

[24] C. McIntyre and W. Grill, "Finite element analysis of the current density and electric field generated by metal microelectrodes," *Ann. Biomed. Eng.,* vol. 29, pp. 227-235, 2001.

[25] D. McCreery, W. Agnew, T. Yuen, and L. Bullara, "Comparison of neural damage induced by electrical stimulation with faradaic and capacitor electrodes," *Ann. Biomed. Eng.,* vol. 16, pp. 463-481, 1988.